

Electron transfer, target excitation, and ionization in $H^+ + Na(3s)$ and $H^+ + Na(3p)$ collisions in the coupled-Sturmian-pseudostate approach

Ashok Jain and Thomas G. Winter

Physics Department, Pennsylvania State University, Wilkes-Barre Campus, Lehman, Pennsylvania 18627

(Received 7 November 1994)

Total cross sections for electron transfer, target excitation, and ionization processes are reported for the $H^+ + Na(3s)$ and $H^+ + Na(3p)$ systems at 1–100 keV impact energies. We have employed a two-center coupled-Sturmian-pseudostate approach that has recently been developed and applied to several quasi-one-electron systems by Winter [Phys. Rev. A **48**, 3706 (1993)]. The Sturmian basis set, together with an analytic Hartree-Fock potential, are chosen carefully so that all three channels (transfer, excitation, and ionization) are represented properly. We also discuss briefly the effects of the binding-energy correction on the calculated cross sections. We find that our various cross sections (σ_{cap}^{tot} , $\sigma_{cap}^{H(n=2)}$, $\sigma_{cap}^{H(2s)}$, $\sigma_{cap}^{H(2p)}$, $\sigma_{exc}^{Na(3s \rightarrow 3p)}$, $\sigma_{exc}^{Na(3s \rightarrow 3d)}$, σ_{ion}^{tot}) and the A_{20} alignment parameter for $Na(3s \rightarrow 3p)$ compare very well with most of the available experimental data, as well as with previous theoretical results. For all the above quantities, when a comparison is made between theory and measurement, our results are equally good or better than the earlier calculations employing different theoretical approaches. We still find a persistent discrepancy between theory (present as well as previous calculations) and measurements for the electron transfer cross sections into the metastable state of the H atom ($\sigma_{cap}^{H(2s)}$). Our results for the orientation and alignment effects in the electron transfer process of $H^+ + Na(3p)$ collisions are in good qualitative accord with recent observations and previous theoretical studies. In particular, we see a strong enhancement for the $H(n \geq 3)$ capture cross sections in the $H^+ + Na(3p)$ collisions. The $H(n=2)$ production cross sections in the $H^+ + Na(3p)$ collisions follow a roughly similar trend, as observed experimentally when plotted against the impact energy.

PACS number(s): 34.70.+e, 34.50.Fa

I. INTRODUCTION

This work is inspired by a recent surge of experimental studies [1–4] on the proton-sodium system to determine the full density-matrix and target excitation cross sections. The final goal of this study is to understand fully the collisional dynamics of the proton-sodium system from low to intermediate energies (1–100 keV). In this first paper, we report total and partial electron transfer (σ_{cap}^{tot} , $\sigma_{cap}^{H(n=1)}$, $\sigma_{cap}^{H(2l)}$, $\sigma_{cap}^{H(3l)}$), target excitation ($\sigma_{exc}^{Na(3s \rightarrow 3p)}$, $\sigma_{exc}^{Na(3s \rightarrow 3d)}$), and ionization (σ_{ion}^{tot}) cross sections in $H^+ + Na(3s)$ collisions at 1–100 keV energies, although most of the previous results (theoretical and experimental) are available only for energies below, roughly, 25 keV. From our $\sigma_{exc}^{Na(3s \rightarrow 3p_0)}$ and $\sigma_{exc}^{Na(3s \rightarrow 3p_1)}$ values we also determine the alignment parameter A_{20} and compare it with experimental and other theoretical data. Further, we will also present cross sections for electron transfer from the aligned and oriented $Na(3p)$ atoms in the 1.5–5 keV impact energy range; these results are compared with recently measured and calculated cross sections.

The proton-sodium system is a prototype quasi-one-electron system, which has been extensively studied in the laboratory for the electron transfer [5–21], target excitation [22–26], and ionization [9] processes. Recently, several measurements and calculations have been performed on the state-selective electron-capture process in proton collisions with aligned and oriented sodium atoms [27–34]. Such collisional studies have many practical ap-

plications in atomic, laser, and plasma physics.

Theoretical calculations on the electron transfer and target excitation processes have been carried out previously from low to intermediate energies by several groups using molecular-orbital (MO) [35–37], augmented atomic-orbital (AO) [30–34, 38–43], and many-body [44] methods. Although there exists good agreement between previous calculations [30–44] and experiments for the total electron transfer cross section, significant discrepancies are found for state-selective electron transfer and target excitation cross sections (see later) when a comparison is made between various previous theoretical results, between different experiments, and between theory and experiment. For example, a large discrepancy between theory and experiment is found for the $\sigma_{cap}^{H(2s)}$ cross section; all the various AO calculations [39–43] differ significantly from each other for the $\sigma_{exc}^{Na(3s \rightarrow 3p)}$ and $\sigma_{exc}^{Na(3s \rightarrow 3d)}$ cross sections. Considerable differences are also observable among several sets of measured cross sections for the $\sigma_{cap}^{H(2p)}$ charge-transfer process. Therefore, it is quite important to carry out another coupled-state calculation for the proton-sodium system where a different basis-set expansion, such as the present Sturmian method, is employed. The ionization cross sections, calculated from the previously augmented AO methods [42,43], also differ from each other both in quantity and quality.

The purpose of the present paper is to apply the coupled-Sturmian-pseudostate approach to the $H^+ + Na(3s)$ and $H^+ + Na(3p)$ collisions from low to in-

intermediate energies (1–100 keV), where an augmented AO method is appropriate in order to properly take into account the coupling between electron transfer, target excitation, and ionization channels. For this system, all three channels are in competition with each other around the 10-keV energy region. Below about 7 keV, the electron transfer process is predominant, while above this energy, target excitation (mainly the $3p$) dominates, followed by the ionization process. An MO expansion is not likely to be suitable at the higher energies. This is a test of the coupled-Sturmian approach for an asymmetric system where a truncated basis set is being used to represent the coupling of all three processes (transfer, excitation, and ionization). Although our ionization cross sections may not be fully converged due to the finite size of the basis set, they will be seen to have good qualitative features.

In Sec. II we summarize our theoretical method, while in Sec. III numerical details are given. In Sec. IV all the cross sections will be presented and compared with experimental data and previous calculations. Concluding remarks will be made in Sec. V. We use atomic units unless otherwise specified.

II. THEORETICAL METHOD

The original approach [45,46] of the coupled-Sturmian-pseudostate method was extended by Winter to arbitrary hydrogenic ion targets [47–49] and to quasi-one-electron targets [50,51] to study electron transfer, ionization, and target excitation processes. A set of Sturmian basis functions is centered on each nucleus, i.e., on the proton (charge $Z_A=1$) and the sodium nucleus (charge $Z_B=11$). The Sturmian function is simply a polynomial multiplied by a fixed exponential $\exp[-\zeta_\alpha r_\alpha/(l_\alpha+1)]$ for a given angular momentum l_α , where r_α is the distance from the nucleus α ($=A$ or B) to the electron, multiplied by a spherical harmonic. The polynomials form a complete set, so the Sturmian method is quite promising.

As discussed earlier [50,51], the two Sturmian charges ζ_α are arbitrary. In the present work, we have tested two different types of analytic Hartree-Fock potentials; namely, the one given by Green, Sellin, and Zachor (GSZ) [52],

$$V(r_B) = \frac{-[(Z_B-1)(Kd\{e^{r_B/d}-1\}+1)^{-1}+1]}{r_B}, \quad (1)$$

and the other given by Shingal *et al.* [40],

$$V(r_B) = -\frac{1}{r_B} - \frac{e^{-3.56r_B}}{r_B} (10 + 17.1r_B). \quad (2)$$

Both of these potentials have the correct asymptotic forms $-Z_B/r_B$ as $r_B \rightarrow 0$ and $-1/r_B$ as $r_B \rightarrow \infty$. For sodium, the values of K and d are given [52] as 2.85 and 0.584, respectively. As usual, the one-electron Hamiltonian of sodium, $-\frac{1}{2}\nabla^2 + V(r_B)$, is diagonalized in the Sturmian basis centered on the nucleus B , and the one-electron Hamiltonian of the hydrogen atom, $-\frac{1}{2}\nabla^2 + V(r_A)$, is diagonalized in the Sturmian basis cen-

tered on nucleus A .

Initially, we started with the GSZ potential [Eq. (1)], with three different sizes of the Sturmian basis: (i), 62 terms ($9sB/9pB/5dB/9sA/6pA/5dA$); (ii), 73 terms ($14sB/9pB/7dB/9sA/6pA/5dA$); and (iii), 77 terms ($14sB/11pB/7dB/9sA/6pA/5dA$), where the notation has an obvious meaning. The higher s , p , and d functions in the 73- and 77-term bases were found to be necessary to produce negative energies for the $n=4$ and $n=5$ states of Na. By varying the value of the Sturmian charge ζ_B arbitrarily, in order to get an energy spectrum as close as possible to the observed values or to the Hartree-Fock limit, we obtained the GSZ eigenvalues as shown in Table I only for the final 77-term Sturmian expansion. With this 77-term Sturmian set (49 functions on the Na center with $\zeta_B=1.5$), we note from Table I that the $3s$ and $3p$ binding energies differ with the experimental values by about 5% and 3%, respectively. The number of coupled equations we solved with 62, 73, and 77 Sturmian functions on both centers is only 55 (excluding $1sB$, $2sB$, $2pB$, $3d_2B$, $4d_2B$, and $5d_2B$), 66 (excluding $1sB$, $2sB$, $13sB$, $14sB$, $2pB$, $9sA$), and 70 (excluding $1sB$, $2sB$, $2pB$, $13sB$, $14sB$, and $9sA$), respectively. At one impact energy (20 keV) and impact parameter ($b=1.0$ a.u.) we checked the sensitivity of various probabilities with respect to the size of the scattering calculation. We found that the 70-state results appear to be converged within 5%. In the following, therefore, we shall discuss only the 70-state results. It is quite interesting that the final cross sections for the present collision system will be seen to be quite sensitive to the accuracy of the $3s$ and $3p$ orbitals of the Na atom.

In an *ad hoc* manner, we then normalized the calculated GSZ [Eq. (1)] $3s$ and $3p$ binding energies to the experimental values and found the binding-energy correction to be significant and to improve the cross sections when compared with the measurements. Before we discuss the effects of binding-energy corrections and different potentials [Eqs. (1) and (2)] on the cross sections, we first summarize the numerical tests on the convergence of the final cross sections.

As described in earlier papers by Winter [50,51], the two-center direct matrix elements of the analytic Hartree-Fock potential [Eq. (1) or (2)] and the two-center

TABLE I. Binding energies (Hartrees) for Na (atom B) using a Sturmian basis. The experimental values are taken from Ref. [58].

Orbital	GSZ [Eq. (1)]	Eq. (2) potential	
	$\zeta_B=1.5$	$\zeta_B=1.3$	Expt.
$3s$	-0.19938	-0.18798	-0.18836
$3p$	-0.10833	-0.10906	-0.1116
$3d$	-0.05594	-0.055617	-0.0559
$4s$	-0.07388	-0.07024	-0.0716
$4p$	-0.049976	-0.049941	-0.051
$4d$	-0.030797	-0.028048	-0.03144
$5s$	-0.02466	-0.00325	-0.0376
$5p$	-0.02753	-0.023345	-0.0292
$5d$	-0.006915	+0.011867	-0.0201

charge-exchange matrix elements of both potentials have been evaluated numerically in prolate spheroidal coordinates over $\lambda = (r_A + r_B)/R$ and $\mu = (r_A - r_B)/R$ (where R is the internuclear distance). The integration over λ was carried out by Gauss-Laguerre quadrature using 16 points in the present energy region of 1–100 keV. The integration over μ was carried out by Gauss-Legendre integration using 32 points at all energies.

As mentioned above, a total of 70 coupled equations were integrated numerically over the variable $z = vt$, using Hamming's method, with the absolute truncation error automatically kept between 5×10^{-6} and 5×10^{-4} at all energies. It had been established earlier by Winter [50,51] that with the use of these limits, the transition probabilities are accurate to 0.2%. In the present collision case, we found that these limits hold good. At the lowest energy (below 2 keV), in order to keep the CPU sec under 2000 per impact parameter, the truncation error limits were increased by a factor of 10 for the small impact parameters only; the errors incurred in various probabilities are within a few percent.

The convergence of the final cross sections was also tested with respect to the range of z and the internuclear separation R beyond which charge-exchange matrix elements are neglected. Varying the value of R between 25.0 and 60.0, we found that with $R = 40.0$ the probabilities are converged to within 0.5%. The overall z integration of the coupled equations was set to be $(-100, 100)$. However, at lower energies (below 5 keV), these limits were changed to $(-100, 500)$. Finally, as mentioned above, we made several tests for the convergence of various cross sections with respect to the total number of channels, i.e., the number of coupled equations. We carried out tests for 55, 66, and 70 states; the final 70-state results are probably converged to within 5%.

Finally, the probabilities have been integrated over the impact parameter b using Simpson's rule. Additional tests were made by employing the trapezoidal rule for the b integration; the two integration schemes agree with each other to within better than 0.5%. We took as many as 26 b points to keep proper convergence of the integral cross sections within a 1% accuracy. Altogether, including basis sensitivity, we believe that our final cross sections are within a 10% accuracy, except for the ionization cross sections, which are probably within a 25% accuracy.

Binding-energy correction and use of different potentials

In Figs. 1 and 2, we have shown our final 70-state $\sigma_{\text{cap}}^{\text{tot}}$ and $\sigma_{\text{exc}}^{3s \rightarrow 3p}$ cross sections for $\text{H}^+ + \text{Na}(3s)$ collisions at 1–20 keV using three versions of the present model: (i), the GSZ potential [Eq. (1)] with binding-energy correction; (ii), the GSZ potential without binding-energy correction for the 3s and 3p orbitals; and (iii), the Eq. (2) potential. We see that using the GSZ potential the 3s and 3p binding-energy corrections are quite large at all energies for these two dominant cross sections for the $\text{H}^+ + \text{Na}(3s)$ collisions. The same is true for other cross sections also (not shown). The present binding-energy correction scheme is quite different from the one dis-

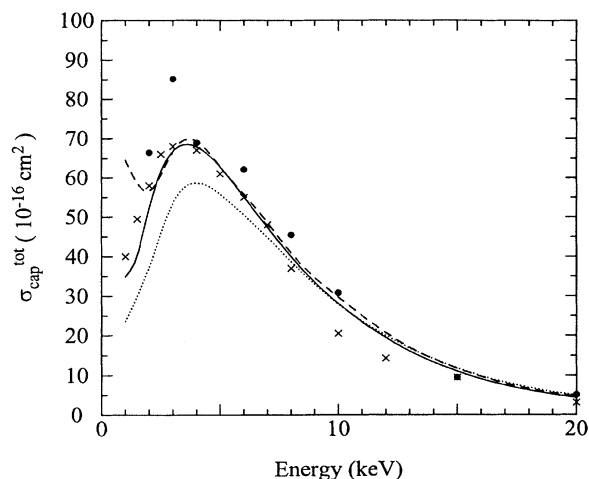


FIG. 1. Effect of the binding-energy correction on the total electron transfer ($\sigma_{\text{cap}}^{\text{tot}}$) cross sections (10^{-16} cm^2) for the $\text{H}^+ + \text{Na}(3s)$ system at 1–25 keV. Present results: solid line, using Eq. (2) potential; dashed curve, GSZ [Eq. (1)] potential with binding-energy correction; dotted curve, GSZ [Eq. (1)] potential without the binding-energy correction. The experimental points are taken from Refs. [10] (crosses) and [15] (solid circles).

cussed by Winter [50,51], in which all target energies were shifted by the same amount. In the present case, we simply replaced the theoretical GSZ 3s and 3p eigenvalues by the corresponding experimental values. Neither scheme is unitary. From Figs. 1 and 2, we find that the cross sections are improved (with respect to experimental data as shown) significantly when such corrections in the values of binding energies of the 3s and 3p orbitals are forced in the scattering calculation. However, this im-

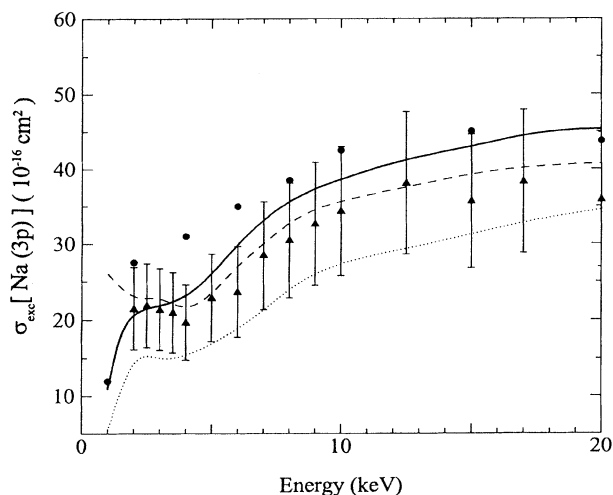


FIG. 2. Same as in Fig. 1, but for target $\text{Na}(3p)$ excitation. Present results: solid line, using the Eq. (2) potential; dashed curve, GSZ [Eq. (1)] potential with binding-energy correction; dotted curve, GSZ [Eq. (1)] potential without the binding-energy correction. Experiment: Ref. [22], solid circles; Ref. [19], solid triangles.

provement in the cross section is not satisfactory at low energies (below 2 keV).

From Figs. 1 and 2, we thus learn that, in order to describe the proton-sodium collision properly, it is quite important that the $3s$ and $3p$ binding energies be as accurate as possible. We wanted to check the hypothesis that this *ad hoc* correction to the $3s$ and $3p$ binding energies might not be suitable in general; for example, for other rather more sensitive cross sections, such as the state-selective electron transfer and the target excitation cross sections to higher n and l values. In order to test this hypothesis, we employed another potential, as given in Eq. (2) above. The values of the Na binding energies using the potential in Eq. (2) are given in Table I, where we clearly see that the difference between calculated and measured values for the dominant $3s$ and $3p$ orbitals is quite small. The $3s-3p$ energy difference using this potential is much closer to the measured value (within 3%) than is that using the GSZ potential. By using the potential in Eq. (2), the $\sigma_{\text{cap}}^{\text{tot}}$ and $\sigma_{\text{exc}}^{3s \rightarrow 3p}$ cross sections are in good agreement with the experimental data. The GSZ results with binding-energy correction are closer to the Eq. (2) values than the ones without this correction; this is true for all other cross sections as well. Our conclusion is the following: a better potential representing the target core should be employed, instead of making *ad hoc* corrections in the binding energies. This preserves unitarity in the coupled equations. Therefore, from now on, in the following discussion, we make use of the Eq. (2) potential to report our final cross sections for all three processes (transfer, excitation, and ionization).

III. RESULTS AND DISCUSSIONS

A. Electron transfer cross sections in $\text{H}^+ + \text{Na}(3s)$ collisions

We now discuss our final cross sections (transfer, excitation, and ionization) using the Eq. (2) potential for the active electron and the Na core. Total electron transfer ($\sigma_{\text{cap}}^{\text{tot}}$) cross sections for collisions between H^+ and $\text{Na}(3s)$ are shown in Fig. 3, along with several sets of experimental data [10,15,18,19]. Also shown in Fig. 3 are the augmented AO calculations of Fritsch [39] and Shingal and Bransden [43]. All the results, theoretical as well as experimental, shown in Fig. 3 are in complete agreement with respect to the energy dependence of $\sigma_{\text{cap}}^{\text{tot}}$. All three AO curves (Fig. 3) are in good accord with each other quantitatively, also. Around the resonance peak (3 keV), present values are slightly higher than the previous AO results [39,43]. All the plotted data in Fig. 3, theoretical as well as experimental, show a peaking structure around 3 keV, which is due to the resonant electron transfer process [matching of projectile velocity with the energy defect of the $\text{H}(n=2)$ electron transfer process]. The measurements of DuBois and Toburen [15] and Aumayr, Lakits, and Winter [19] differ significantly from each other in the 1–10 keV region. Our $\sigma_{\text{cap}}^{\text{tot}}$ values are in excellent agreement with the measurements of Anderson *et al.* [10] at all energies shown in Fig. 1, except possibly at the highest energy. Above 25 keV (not shown, but given in Table II), the $\sigma_{\text{cap}}^{\text{tot}}$ values decrease rapidly

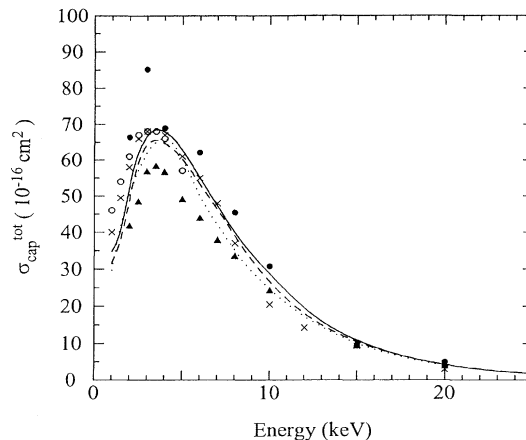


FIG. 3. Total electron transfer cross sections ($\sigma_{\text{cap}}^{\text{tot}}$) (10^{-16} cm^2) for the $\text{H}^+ + \text{Na}(3s)$ system in the laboratory-frame energy range of 1–25 keV. Theory: present coupled-Sturmian results, solid curve; dashed curve, Shingal and Bransden [43]; dotted curve, Fritsch [39]. Experiment: Anderson, Howald, and Anderson [10] (crosses); DuBois and Toburen [15] (solid circles); Ebel and Salzborn [18] (open circles); Aumayr *et al.* [19] (solid triangles).

with an increase in energy. However, above 25 keV there is a large discrepancy between present theory and the measurements of DuBois and Toburen [15] for $\sigma_{\text{cap}}^{\text{tot}}$; for example, the present theoretical values (in units of 10^{-16} cm^2) of 0.079 and 0.0077 at 60 and 100 keV, respectively, are very small compared to their measured values of 0.575 and 0.363, respectively. The AO results of Shingal and Bransden [43] in the 25–50 keV region are also much smaller than the experimental data of Ref. [15]. The reason for this rather large discrepancy between theory and experiment is not clear.

The state-selective electron transfer cross sections to the $\text{H}(2s)$ and $\text{H}(2p)$ states are shown in Figs. 4 and 5, respectively. For the $\text{H}(2s)$ case (Fig. 4), there is a large discrepancy between coupled-state (augmented AO) results (present, Fritsch [39] and Shingal and Bransden [43]) and the measured values of Berkowitz and Zorn [14] (1–2.5 keV) and Nagata and Kuribara [16] (1–5 keV). The two measurements [14,16] also differ significantly from each other. However, the augmented AO values, shown in Fig. 4, are higher than the measurements by about a factor of 2.5 in the resonance region. It is, however, interesting to notice that the 3-keV peak, observed by Nagata and Kuribara [16], is present in the theoretical results. It may be possible that the measurements involve large errors in their absolute values. Near the peak (3 keV), the augmented AO results are in agreement to within 15%. More recent coupled-state calculations [30,33] (not shown) for the $\text{H}(2s)$ production in $\text{H}^+ + \text{Na}(3s)$ collisions also confirm this large discrepancy between coupled-state theory and the measurements of Refs. [14] and [16]. On the other hand, the many-body calculations of Avakov *et al.* [44] seem to have good agreement with experiments [14,16] for the $\text{H}(2s)$ production in $\text{H}^+ + \text{Na}(3s)$ collisions. The MO calculations of Allan [37] (not shown) for the $\text{H}(2s)$ transfer cross sec-

TABLE II. Present 70-state cross sections (10^{-16} cm^2) and alignment parameter [using Eq. (2) potential] for $\text{H}^+ + \text{Na}(3s)$ collisions.

Energy (keV)	$\sigma_{\text{cap}}^{\text{tot}}$	$\sigma_{\text{cap}}^{\text{H}(2s)}$	$\sigma_{\text{cap}}^{\text{H}(2p)}$	$\sigma_{\text{cap}}^{\text{H}(n=3)}$	$\sigma_{\text{exc}}^{3s \rightarrow 3p}$	$\sigma_{\text{exc}}^{3s \rightarrow 3d}$	A_{20}
1.0	34.84	11.50	19.49	2.09	10.96	1.45	-0.482
1.5	40.30	15.72	20.83	2.51	17.90	1.09	-0.399
2.0	52.25	20.72	26.77	3.69	20.61	1.10	-0.514
3.0	66.75	24.82	35.14	5.61	21.90	0.66	-0.616
4.0	67.89	23.30	35.99	6.82	23.20	0.74	-0.486
5.0	62.77	19.60	32.70	7.73	26.06	1.30	-0.360
6.0	55.11	15.81	27.67	7.81	29.83	2.12	-0.296
7.0	47.33	12.54	22.48	7.77	33.14	2.94	-0.260
8.0	39.92	9.71	18.27	7.18	35.61	3.63	-0.230
10.0	28.08	5.80	11.37	6.11	38.60	4.34	-0.179
12.5	17.67	3.10	6.35	4.39	41.18	4.73	-0.115
15.0	10.94	1.74	3.52	2.88	42.99	4.72	-0.065
17.5	6.80	1.02	2.07	1.74	44.68	4.79	-0.039
20.0	4.28	0.61	1.24	1.28	45.29	4.81	-0.029
25.0	1.75	0.23	0.47	0.46	44.38	4.68	-0.039
30.0	0.80	0.086	0.228	0.195	40.84	4.50	-0.035
40.0	0.26	0.017	0.093	0.05	33.84	3.32	+0.054
50.0	0.135	0.01	0.049	0.025	31.11	2.36	+0.074
60.0	0.079	0.007	0.025	0.016	28.92	1.98	+0.073
80.0	0.023	0.002	0.0064	0.0056	24.55	1.54	+0.099
100.0	0.0077	0.0008	0.0021	0.0013	21.57	1.19	+0.117

tions agree more closely with the augmented AO values than the results of Avakov *et al.* [44]. Thus, this large discrepancy between theory and experiment for the $\text{H}(2s)$ cross sections remains to be resolved.

In Fig. 5, the present $\text{H}(2p)$ charge-transfer cross sections are compared with the measurements of Gieler *et al.* [21], Finck *et al.* [20], and Nagata and Kuribara [16]. We see an excellent agreement, both in quality and quantity, between present theory and the most recent

measurement (Gieler *et al.* [21]). Also shown in Fig. 5 are the augmented AO calculations of Shingal and Bransden [43], which are also in excellent agreement with our cross sections. The measurements of Nagata and Kuribara [16] are too low (by almost a factor of 2) as compared to the other two measurements [20,21]. Here, we have not shown the augmented AO results of Fritsch [39], MO calculations [35–37], recent augmented AO values of Refs. [30] and [33], and finally the many-body

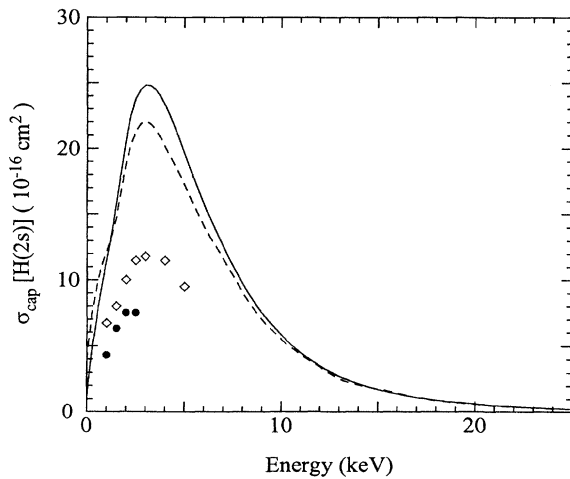


FIG. 4. Electron transfer cross sections (10^{-16} cm^2) into $\text{H}(2s)$ for impact of H^+ on $\text{Na}(3s)$ in the laboratory-frame energy range of 1–25 keV. Theory: present, solid curve; dashed curve, Shingal and Bransden [43]. Experiment: Berkowitz and Zorn [14] (solid circles); Nagata and Kuribara [16] (open squares).

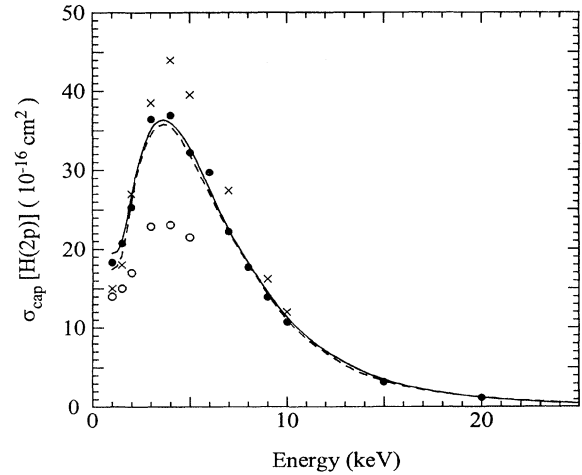


FIG. 5. Electron transfer cross sections (10^{-16} cm^2) into $\text{H}(2p)$ for impact of H^+ on $\text{Na}(3s)$ in the laboratory-frame energy range of 1–25 keV. Theory: present, solid curve; dashed curve, Shingal and Bransden [43]. Experiment: Finck *et al.* [20] (crosses); Nagata and Kuribara [16] (open circles); Gieler *et al.* [21] (solid circles).

values of Ref. [44]. However, the agreement among these results and the present results is good. It is interesting to note that for the H(2s) case (Fig. 4), the measurements of Nagata and Kuribara [16] are also lower by almost a factor of 2. Thus, if we assume (on the basis of Fig. 5) that in general the experiment of Nagata and Kuribara [16] can be normalized by about factor of 2, the H(2s) curves in Fig. 4 will show a better agreement between theory and experiment.

Finally, in Fig. 6, we compare our cross sections for capture into various n shells of the H atoms ($\sigma_{\text{cap}}^{n=11}$, $\sigma_{\text{cap}}^{n=2}$, $\sigma_{\text{cap}}^{n=3}$) over the whole range of present impact energies (1–100 keV). Capture to the $n=2$ shell dominates the entire range. The next dominant electron transfer channel is into the $n=3$ shell. Electron transfer to the $n=1$ shell is small at all energies considered here (although presumably it dominates at high energies). However, we shall see later that in the aligned and oriented state of the Na(3p) atom, it is the $n=3$ shell that is preferred at low energies.

In a further attempt to compare our calculations with the measurements, we plot in Fig. 7 the metastable fraction $f_{2s} = \sigma_{\text{cap}}^{2s} / \sigma_{\text{cap}}^{n=2}$, which has been measured directly by Nagata [11] in the low-energy region (1–5 keV). Such a comparison has also been made by Allan [37] in his MO theory. From Fig. 7, we see a qualitative agreement between theory and experiment; the 2 keV peaking behavior, observed by Nagata, is reproduced by our theoretical curve. Quantitatively, again, we find that the observed data are lower by almost a factor of 2. It seems that the discrepancy of about a factor of 2 in the measurements of Nagata is present in all the three sets of electron-capture results, as discussed above.

B. Target excitation cross sections in $\text{H}^+ + \text{Na}(3s)$ collisions

The Na(3p) excitation is the dominant channel in proton collisions with sodium atoms in the present energy region. Figure 8 shows our cross sections for the excitation of the Na(3p) states in the energy range 1–25 keV. We have shown our results with and without cascading

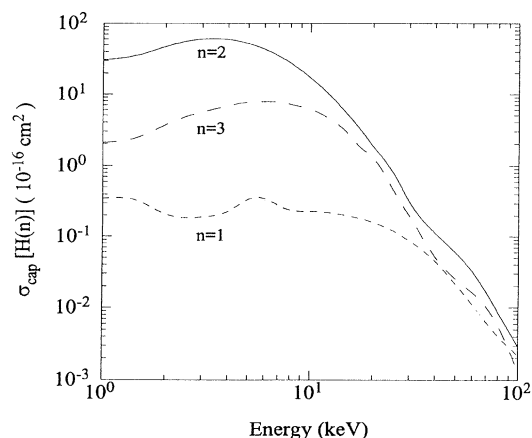


FIG. 6. Electron transfer cross sections (10^{-16} cm^2) into $\text{H}(n=1)$, $\text{H}(n=2)$, and $\text{H}(n=3)$ for impact of H^+ on $\text{Na}(3s)$ in the laboratory-frame energy range of 1–25 keV.

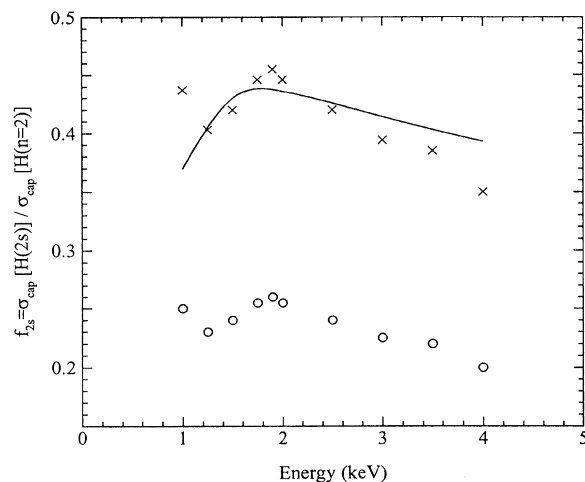


FIG. 7. Metastable fraction, $f_{2s} = \sigma_{\text{cap}}[\text{H}(2s)] / \sigma_{\text{cap}}[\text{H}(n=2)]$, in H^+ collisions with $\text{Na}(3s)$ atoms at 1–5 keV. Present calculations are plotted as a solid line, while the experimental points of Nagata [11] are shown as open circles and crosses (multiplied by a factor of 1.75).

effects. For this transition, the cascading effects are within 12–25 % in this energy range. Also shown in Fig. 8 are the augmented AO results of Fritsch [42] and Shingal and Bransden [43]. The experimental points are taken from Howald *et al.* [22] (1–25 keV); Lavrov and Lomsadze [24] (1–14 keV); Jitschin *et al.* [25] (1–6 keV); and Aumayr, Lakits, and Winter [19] (1–20 keV). First, we notice that all these measurements involve absolute errors of the order of 40%. For clarity, errors bars are shown only for the experimental data of Ref. [19]. Our results,

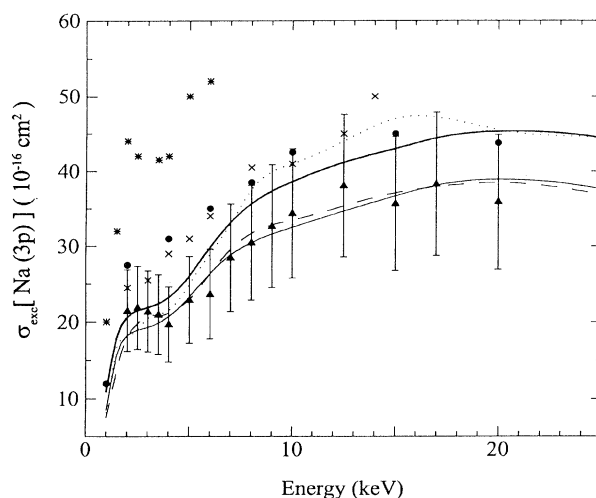


FIG. 8. Na(3p) excitation cross sections (10^{-16} cm^2) for the $\text{H}^+ + \text{Na}(3s)$ system at 1–25 keV. Present results: thick solid curve (with cascade effects); thin solid curve (without cascade effects). The calculations of Fritsch [42] (dotted line) include cascade effects, while the results of Shingal and Bransden [43] (dashed curve) are plotted without cascade effects. Experiment: Ref. [22], solid circles; Ref. [24], crosses; Ref. [25], stars; Ref. [19], solid triangles.

including cascade effects, compare very well with all the measurements, except the values of Jitschin *et al.* [25], which were taken only up to 6 keV. The data of Jitschin *et al.* [25] are widely discrepant from the other three [19,23,24] measured values. From Fig. 8 we also see that our results are in fair agreement with the augmented AO calculations of Fritsch [42] (including cascading effects). The overall impact energy dependence of the Na(3p) excitation cross section is quite similar in all three of the augmented AO curves and the measurements. A shoulder between 2 and 3 keV is seen in almost all the data depicted. From the energy dependence of the excitation cross section we see that, in addition to the 2-keV shoulder, there is another broad structure (enhancement in the cross section) between 15 and 20 keV; this seems also to be the case in previous AO results [42,43] and in the experimental points [19,23]. The energy defect $\Delta E = 2.1$ eV ($v_e \approx 0.39$ a.u.) of the $3s \rightarrow 3p$ transition corresponds quite closely to the projectile velocity ($0.28 \sim 0.35$) at the 2–3 keV impact energy.

In order to see further the quality of the Na(3p) excitation cross section, we plot in Fig. 9 the orientation and alignment parameter A_{20} along with the measurements of Jitschin *et al.* [25] and the augmented AO results of Fritsch [42] and Shingal and Bransden [43]. It is interesting to note that in the low-energy region (1–6 keV), where the measurements are available, there is excellent agreement among all three of the augmented AO results and the observed data [25], although the Na(3p) excitation cross sections of Jitschin *et al.* [25] have been seen to be widely discrepant from all the other data (theoretical and experimental) depicted in Fig. 8. The agreement of the MO calculation of Allen [37] (not shown) is not even qualitative, nor do the Born-type theories [53] (not shown) give reasonably good results. The Na(3p) excitation is influenced mainly by the electron transfer channel,

which is properly considered in the present model. It is also established by the Born-type calculations for the A_{20} parameter that the excitation of the Na core plays no important role for the Na(3p) excitation process (see Ref. [25]). Thus the importance of charge-transfer channels in the AO treatment is quite clear. In addition, coupling of the higher Na and H states to the Na ($3s \rightarrow 3p$) transition plays an important role. The measured apparent cross sections include all the cascades feeding the Na(3p) population. All of these important factors have been accounted for in the present results shown in Figs. 8 and 9. The minimum around 3 keV in the measured A_{20} values and the apparent tendency towards zero at higher energies are in excellent agreement with all the AO curves as shown in Fig. 9; however, experiments above 10 keV would be of value to confirm this tendency.

We now compare in Fig. 10 our Na(3d) excitation cross sections with other augmented AO results [42,43] and with the only available measurements (Allen, Anderson, and Lin [26]) in the energy range of 1–25 keV. The cascade effects for this transition are very small. Here, we see a large discrepancy between the present results and the augmented AO results of Fritsch [42], which exhibit several peaks in this energy range; such structures in the cross section versus energy are not present in the experimental results of Allen, Anderson, and Lin [26]. We can clearly see that the present results compare better than the other two AO results with the observed values. The results of Shingal and Bransden [43] exhibit a peak around 2 keV in the Na(3d) cross section, which is suggested in our calculations also. This 2 keV structure in the Na(3d) channel may be an indication of a strong coupling of the excitation channel with the H($n=2$) charge-transfer channel. The same may be true for the Na(3p) case (see Fig. 8).

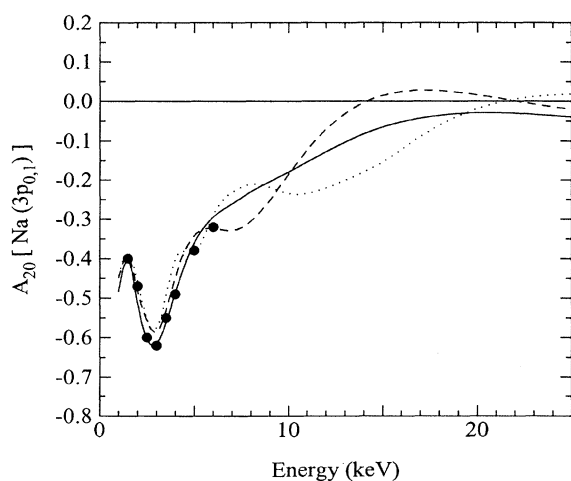


FIG. 9. Na(3p) alignment parameter (A_{20}) in collisionally induced Na($3s \rightarrow 3p$) excitation by proton impact. Theoretical results: present, solid curve; dashed curve, Ref. [43]; dotted curve, Ref. [42]. The experimental data (solid circles) are from Ref. [25].

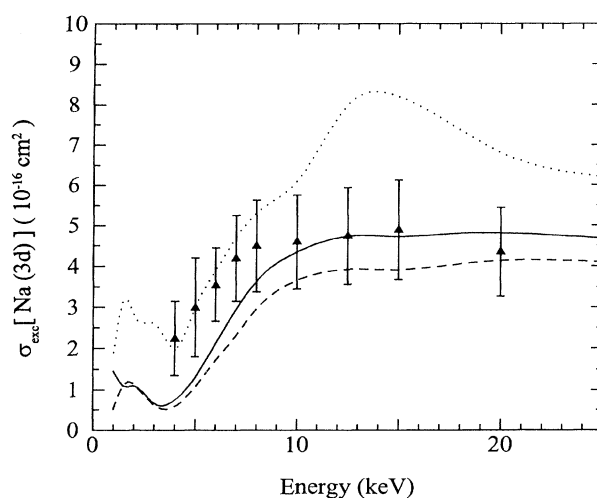


FIG. 10. Na(3d) excitation cross sections (10^{-16} cm^2) for the $\text{H}^+ + \text{Na}(3s)$ system at 1–25 keV. Theory: present results, solid line; Fritsch [42], dotted line; Shingal and Bransden [43], dashed curve. Experiment: Allen, Anderson, and Lin [26], solid triangles.

C. Ionization cross sections in $H^+ + Na(3s)$ collisions

To the best of our knowledge, there are no measurements of ionization cross sections for proton collisions with sodium atoms in the low-energy (below 25 keV) region. Above 20 keV, O'Hare, McCullough, and Gilbody [9] have measured total ionization cross sections for the proton-sodium system. At low energies, however, it would be interesting to compare the electron and proton impact ionization of Na atoms at equal projectile velocities. Experimental [54] and close-coupling [55] data for the electron-Na ionization cross sections are available in the 0.5–2.0 a.u. velocity region. In Fig. 11, we compare electron and proton impact ionization cross sections in the 0.5–2.0 a.u. projectile velocity range. It is quite interesting that there is at least qualitative agreement between electron and proton data. In Fig. 12, we have plotted our total ionization cross section for the $H^+ + Na(3s)$ collisions along with the augmented AO results of Fritsch [42] and Shingal and Bransden [43]. The 15-keV broad enhancement in the energy dependence of the total ionization cross section is present in all three AO results. We also see a 2-keV peak in our results. Measurements of this cross section would be of value.

In the present energy region (1–100 keV), it is interesting to make a comparison of total electron transfer, target excitation, and ionization cross sections. It is seen in Fig. 13 that below 10 keV, charge transfer (mostly into the $n=2$ shell) dominates, while target excitation (mostly $3s$ to $3p$) dominates in the 7–100 keV region. The electron transfer cross sections are very small above 25 keV as compared to excitation and ionization channels. Around the 5–15 keV region, all three processes are strongly coupled and competitive with each other. Finally, in Table II we provide numerical values of several cross sections in the 1–100 keV region obtained from our 70-state Sturmian calculation.

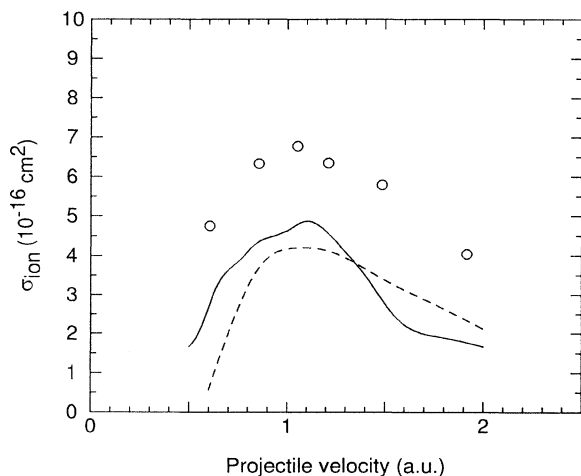


FIG. 11. $H^+ + Na(3s)$ ionization cross sections (10^{-16} cm^2) for electron and proton impact as a function of projectile velocity. Solid curve, present proton results. Dashed curve, theoretical results for electron impact by Bray [55]. Experimental points for electron impact are from Ref. [54].

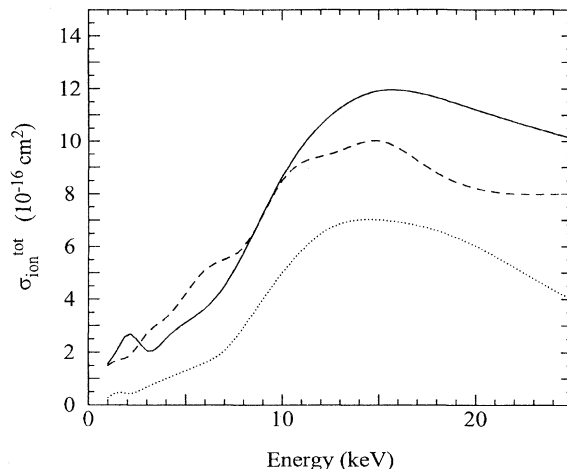


FIG. 12. Total ionization cross sections (10^{-16} cm^2) for the $H^+ + Na(3s)$ system at 1–25 keV. Theory: present results, solid line; Fritsch [42], dotted line; Shingal and Bransden [43], dashed curve.

D. Electron-capture cross sections in $H^+ + Na(3p)$ collisions

As mentioned above, there are several measurements on capture into $H(nl)$ states in H^+ collisions with oriented and aligned $Na(3p)$ atoms. Such effects have been found to be very large in the low-energy (1–5 keV) region [27–34]. In the present model, it is easy to study such effects by simply changing the initial conditions of the unknown amplitudes in the solution of the coupled equations. Unlike the $H^+ + Na(3s) \rightarrow H(n=2) + Na^+$ case (where the energy defect of -1.74 eV implies an endothermic process), the $H^+ + Na(3p) \rightarrow H(n=2) + Na^+$ collision is exothermic (defect $+0.36 \text{ eV}$). The number of calculations for the $H^+ + Na(3p)$ system is rather limited. For this collision system, we have limited our energy range from 1.5 to up to 5 keV only. It was first predicted by Allan, Shingal, and Flower [56] that the $H(2p)$ cross

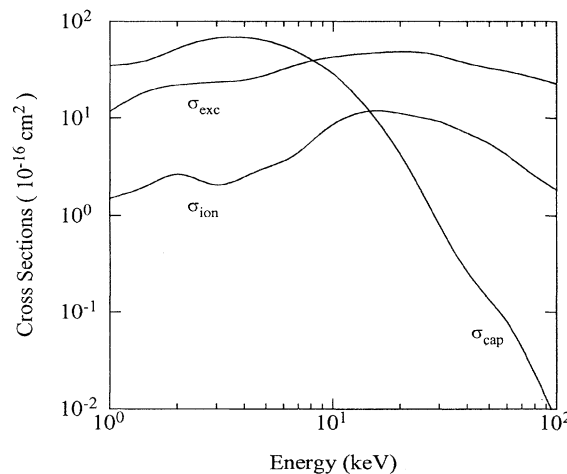


FIG. 13. A comparison of total electron transfer, target excitation, and total ionization cross sections for the $H^+ + Na(3s)$ collisions in the present energy region of 1–100 keV.

TABLE III. Total cross sections (10^{-16} cm^2) [using Eq. (2) potential] for $\text{H}(2s)$ and $\text{H}(2p)$ capture from the different initial states $\text{Na}(3s)$, $\text{Na}(3p_0)$, and $\text{Na}(3p_1)$.

keV	From To	3s		3p ₀		3p ₁	
		2s	2p	2s	2p	2s	2p
1.5	a	15.7	20.8	13.4	66.3	5.2	51.3
	b	14.5	23.7	17.3	71.4	3.3	48.8
	c	16.7	21.1	17.0	57.8	2.8	50.0
	d	17.3	21.9	26.6	49.6	8.9	56.7
2.0	a	20.7	26.8	17.0	60.5	4.3	49.1
	b	22.6	29.9	19.1	60.3	2.6	42.8
	d	18.0	25.9	28.2	42.0	7.6	54.1
3.0	a	24.8	35.1	11.9	45.8	4.3	40.5
	b	22.9	27.9	14.7	45.9	2.1	34.2
	c	23.5	32.8	14.0	44.1	2.4	38.4
	d	17.9	34.2	26.8	36.9	6.2	49.3
5.0	a	19.6	32.7	3.2	34.2	3.3	23.3
	b	20.7	29.0	5.7	33.2	0.8	16.1
	c	17.4	31.3	3.6	30.7	1.9	21.6
	d	15.6	37.1	18.8	33.1	4.6	41.3

^aPresent calculations.

^bDuBois, Nielsen, and Hansen [33].

^cFritsch [57].

^dCourbin *et al.* [30].

sections are quite large when the Na target is prepared in the $3p$ excited state for collision energies between 1 and 20 keV. This trend in the $\text{H}(2p)$ cross section was confirmed in recent $\text{H}^+ + \text{Na}(3p)$ measurements [19]. Later, alignment effects were measured for the $\text{H}(n=2)$ and $\text{H}(n=3, n>3)$ transfer cross sections below 5 keV energy [27,28].

As a first step, in this paper, we report total electron transfer cross sections into $\text{H}(nl)$ states in the $\text{H}^+ + \text{Na}(3p)$ collisions at 1.5–5 keV. In Table III, we provide our $\text{H}(2s)$ and $\text{H}(2p)$ cross sections from $\text{Na}(3s)$, $\text{Na}(3p_0)$, and $\text{Na}(3p_1)$ states along with calculations of

Fritsch [57]; Courbin *et al.* [30]; and DuBois, Nielsen, and Hansen [33]. Although there are quantitative discrepancies among these AO calculations, the trend of the electron transfer cross sections from $\text{Na}(3s)$ and $\text{Na}(3p)$ states as a function of energy is quite similar. For example, in agreement with experiments [27,28], these theoretical results (including ours) given in Table III predict a preference for capture from the initial oriented state $[\text{Na}(3p)]$ in this low-energy region. The measurements of Finck *et al.* [20] for the $\text{H}(2p)$ capture found that there is strong enhancement in collisions of H^+ with laser excited $\text{Na}(3p)$ over $\text{Na}(3s)$ at energies be-

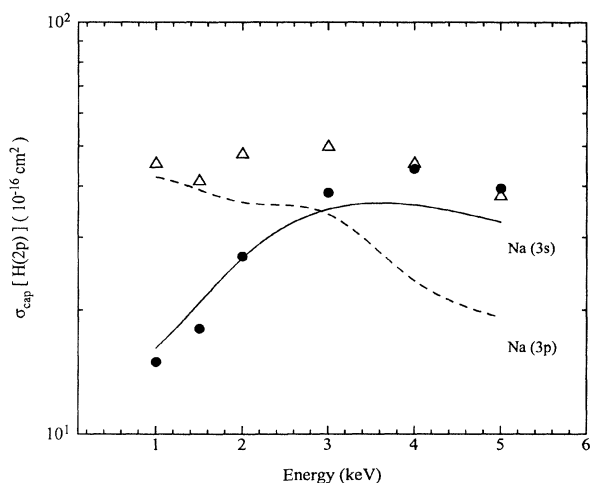


FIG. 14. Effects of orientation and alignment of Na atoms on the electron transfer cross sections into the $\text{H}(2p)$ state. Present results: solid curve, initial $\text{Na}(3s)$ state; dashed curve, initial $\text{Na}(3p)$ state. The experimental data are from Ref. [27]: solid circles, initial $\text{Na}(3s)$; open triangles, initial $\text{Na}(3p)$.

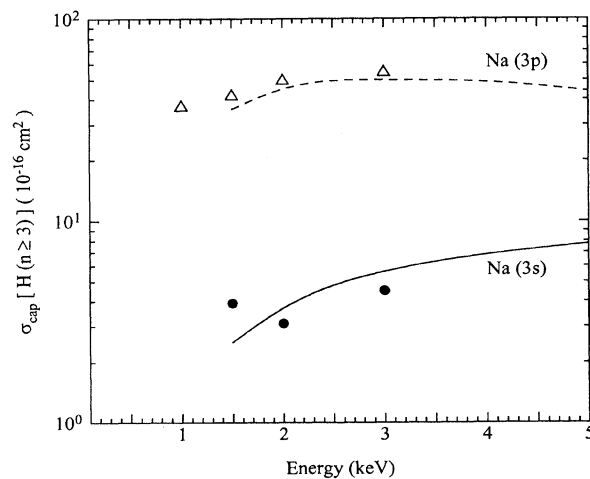


FIG. 15. Effects of orientation and alignment of Na atom on the electron transfer cross sections into the $\text{H}(n \geq 3)$ state. Present results: solid curve, initial $\text{Na}(3s)$ state; dashed curve, initial $\text{Na}(3p)$ state. The experimental data are from Ref. [27]: solid circles, initial $\text{Na}(3s)$; open triangles, initial $\text{Na}(3p)$.

tween 0.5 and 3 keV. This is consistent with our results shown in Table III. A comparison of theory and experiment for $H(2p)$ capture from the $Na(3p)$ state is shown in Fig. 14 along with capture from $Na(3s)$, where we see that the agreement between present theory and experiment is not satisfactory, except below 2 keV.

Finally, Fig. 15 illustrates our results for capture to $H(n \geq 3)$ from $Na(3s)$ and $Na(3p)$ states along with the measured values of Royer *et al.* [27]. There is good agreement between theory and experiment for both $H^+ + Na(3s)$ and $H^+ + Na(3p)$ collisions.

IV. CONCLUSIONS

A 70-state coupled-Sturmian-pseudostate approach has been employed to calculate electron transfer, target excitation, and ionization cross sections for $H^+ + Na(3s)$ and $H^+ + Na(3p)$ collisions in the 1–100 keV energy region. Although we found that it is essential to enforce binding-energy corrections, in our final results we have avoided any binding-energy correction by employing an analytic Hartree-Fock potential that gives quite accurate eigenvalues for the predominant $3s$ and $3p$ Na orbitals using the finite Sturmian expansion. Present cross sections for total electron transfer, state-selective electron transfer [$H(nl)$], and target excitation from $Na(3s)$ to $Na(3p)$ and $Na(3d)$ have been shown graphically along with other theoretical and experimental data in the 1–25 keV range.

Above 25 keV, all of these cross sections have also been tabulated. We found that the present Sturmian AO method is quite successful in describing $H^+ + Na(3s)$ and $H^+ + Na(3p)$ collisions in the present energy region. In particular, our results for total electron transfer, $H(2p)$ production, and excitation to $Na(3p)$ (including the alignment parameter A_{20}) and $Na(3d)$ states are in good agreement with the measured data. The large discrepancy, observed earlier, between theory and experiment for the $H(2s)$ cross section still persists. Our ionization cross sections are in qualitative agreement with the corresponding electron impact data at equal projectile velocities. Altogether, the present calculations reproduce almost all the salient features observed in various processes for the $H^+ + Na(3s)$ collisions. A 2–3 keV enhancement, in almost all the cross sections, is found to exist for the present collision system. The target orientation effects on the electron transfer cross sections [$H(nl)$] are faithfully reproduced in the present work.

ACKNOWLEDGMENTS

We would like to thank Professor Steven Alston for helpful discussions. This work was supported by the U. S. Department of Energy, Office of Energy Research, Office of Basic Energy Sciences, Division of Chemical Sciences. These calculations were performed on Pennsylvania State University's IBM ES9000-740 computer.

-
- [1] C. Richter, N. Anderson, J. C. Brenot, D. Doweck, J. C. Houver, J. Salgado, and J. W. Thomsen, *J. Phys. B* **26**, 723 (1993).
 - [2] Z. Roller-Lutz, Y. Wang, K. Finck, and H. O. Lutz, *J. Phys. B* **26**, 2697 (1993).
 - [3] J. C. Houver, D. Doweck, and C. Richter, *Phys. Rev. Lett.* **68**, 162 (1992).
 - [4] D. Doweck, J. C. Houver, J. Pommier, C. Richter, and T. Royer, *Phys. Rev. Lett.* **64**, 1713 (1990).
 - [5] W. Gruebler, P. A. Schelzback, V. Konig, and P. Marmier, *Helv. Phys. Acta* **43**, 254 (1970).
 - [6] B. A. D'jachkov, V. I. Zinenko, and M. A. Paulii, *Zh. Tekh. Fiz.* **41**, 2353 (1971) [*Sov. Phys. Tech. Phys.* **16**, 1868 (1972)].
 - [7] G. I. Dimov and G. V. Roslyakov, *Instrum. Exp. Tech. (USSR)* **17**, 658 (1974).
 - [8] R. N. Il'in, V. A. Oparin, E. S. Solov'ev, and N. V. Fedorenko, *Zh. Tekh. Fiz.* **36**, 1241 (1965) [*Sov. Phys. Tech. Phys.* **11**, 921 (1967)].
 - [9] B. G. O'Hare, R. W. McCullough, and H. B. Gilbody, *J. Phys. B* **8**, 2968 (1975).
 - [10] C. J. Anderson, A. M. Howald, and L. W. Anderson, *Nucl. Instrum. Methods* **165**, 583 (1979).
 - [11] T. Nagata, *J. Phys. Soc. Jpn.* **46**, 1622 (1979).
 - [12] T. Nagata, *J. Phys. Soc. Jpn.* **48**, 2068 (1980).
 - [13] T. Nagata, *Mass Spectrosc.* **30**, 153 (1982).
 - [14] J. K. Berkowitz and J. C. Zorn, *Phys. Rev. A* **29**, 611 (1984).
 - [15] R. D. DuBois and L. H. Toburen, *Phys. Rev. A* **31**, 3603 (1985).
 - [16] T. Nagata and M. Kuribara, *J. Phys. Soc. Jpn.* **55**, 500 (1986).
 - [17] F. Aumayr and H. Winter, *J. Phys. B* **20**, L803 (1987).
 - [18] F. Ebel and E. Salzborn, *J. Phys. B* **20**, 4531 (1987).
 - [19] F. Aumayr, G. Lakits, and H. Winter, *J. Phys. B* **20**, 2025 (1987).
 - [20] K. Finck, Y. Wang, Z. Roller-Lutz, and H. O. Lutz, *Phys. Rev. A* **38**, 6115 (1988).
 - [21] M. Gieler, F. Aumayr, P. Ziegelwanger, H. Winter, and W. Fritsch, *Phys. Rev. A* **43**, 127 (1991).
 - [22] A. M. Howald, R. E. Miers, J. S. Allen, L. W. Anderson, and C. C. Lin, *Phys. Lett.* **92A**, 328 (1982).
 - [23] A. M. Howald, L. W. Anderson, and C. C. Lin, *Phys. Rev. Lett.* **51**, 2029 (1983).
 - [24] V. M. Lavrov and R. A. Lomsadze, in *Abstracts of Contributed Papers, Thirteenth International Conference on the Physics of Electronic and Atomic Collisions, Berlin, 1983*, edited by J. Eichler, W. Fritsch, I. V. Hertel, N. Stolterfoht, and U. Wille (North-Holland, Amsterdam, 1984).
 - [25] W. Jitschin, S. Osimitsch, D. W. Mueller, H. Reihl, R. J. Allan, O. Schöller, and H. O. Lutz, *J. Phys. B* **19**, 2299 (1986).
 - [26] James S. Allen, L. W. Anderson, and C. C. Lin, *Phys. Rev. A* **37**, 349 (1988).
 - [27] T. Royer, D. Doweck, J. C. Houver, J. Pommier, and N. Andersen, *Z. Phys. D* **10**, 45 (1988).
 - [28] C. Richter, D. Doweck, J. C. Houver, and N. Andersen, *J. Phys. B* **23**, 3925 (1990).
 - [29] M. Gieler, F. Aumayr, M. Hüttenecker, and H. Winter, *J. Phys. B* **24**, 4419 (1991).
 - [30] C. Courbin, R. J. Allan, P. Salas, and P. Wahnnon, *J. Phys. B* **23**, 3909 (1990).

- [31] A. DuBois, J. P. Hansen, M. Lundsgaard, and S. E. Nielsen, *J. Phys. B* **24**, L269 (1991).
- [32] E. Lewartowski and C. Courbin, *J. Phys. B* **25**, L63 (1992).
- [33] A. DuBois, S. E. Nielsen, and J. P. Hansen, *J. Phys. B* **26**, 705 (1993).
- [34] E. Lewartowski and C. Courbin, *J. Phys. B* **26**, 3403 (1993).
- [35] C. Kubach and V. Sidis, *Phys. Rev. A* **23**, 110 (1981).
- [36] M. Kimura, R. E. Olson, and J. Pascale, *Phys. Rev. A* **26**, 1138 (1982).
- [37] R. J. Allan, *J. Phys. B* **19**, 321 (1986).
- [38] R. J. Bell and B. G. Skinner, *Proc. Phys. Soc. London* **80**, 404 (1962).
- [39] W. Fritsch, *Phys. Rev. A* **30**, 1135 (1984).
- [40] R. Shingal, B. H. Bransden, A. M. Ermolaev, D. R. Flower, C. W. Newby, and C. J. Nobel, *J. Phys. B* **19**, 309 (1986).
- [41] R. Shingal and B. H. Bransden, *J. Phys. B* **20**, L127 (1987).
- [42] W. Fritsch, *Phys. Rev. A* **35**, 2342 (1987).
- [43] R. Shingal and B. H. Bransden, *J. Phys. B* **20**, 4815 (1987).
- [44] G. V. Avakov, L. D. Blokhintsev, A. S. Kadyrov, and A. M. Mukhamedzhanov, *J. Phys. B* **25**, 213 (1992).
- [45] D. F. Gallaher and L. Wilets, *Phys. Rev.* **169**, 139 (1968).
- [46] R. Shakeshaft, *Phys. Rev. A* **14**, 1626 (1976).
- [47] T. G. Winter, *Phys. Rev. A* **25**, 697 (1982).
- [48] T. G. Winter, *Phys. Rev. A* **35**, 3799 (1987).
- [49] T. G. Winter, *Phys. Rev. A* **33**, 3842 (1986).
- [50] T. G. Winter, *Phys. Rev. A* **47**, 264 (1993).
- [51] T. G. Winter, *Phys. Rev. A* **48**, 3706 (1993).
- [52] A. E. S. Green, D. L. Sellin, and A. S. Zachor, *Phys. Rev.* **184**, 1 (1969).
- [53] O. Schöller and S. J. Briggs, *Fundamental Processes in Atomic Collision Physics*, edited by Kleinpoppen *et al.* (Plenum, New York, 1985).
- [54] I. P. Zapesochnyi and I. S. Aleksakhin, *Zh. Eksp. Teor. Fiz.* **55**, 76 (1968) [*Sov. Phys. JETP* **28**, 41 (1969)].
- [55] I. Bray, *Phys. Rev. Lett.* **73**, 1088 (1994).
- [56] R. J. Allan, R. Shingal, and D. R. Flower, *J. Phys. B* **19**, L251 (1986).
- [57] W. Fritsch, as quoted in Ref. [33].
- [58] C. E. Moore, *Atomic Energy Levels*, Natl. Bur. Stand. Ref. Data Ser., Natl. Bur. Stand. (U.S.) Circ. No. 35 (U.S. GPO, Washington, DC, 1949), Vol. I.